Journal of Petroleum Science and Technology 12(3): 35, 2022, Pages 24-36
DOI:10.22078/JPST.2023.4572.1755

Journal of Petroleum Science and Technology
Research Paper
https://jpst.ripi.ir/

Simulation of Asphaltene Precipitation in the Reservoir and Its Final Effect on Wells' Productivity Index

Sedigheh Izadi* and Mohammad Jafarzadegan
Engineering Department, National Iranian South Oil Company, Ahwaz, Iran

Abstract
Asphaltene precipitation causes a decrease in the effective mobility of hydrocarbon through pore throats plugging and, as a result, the rock permeability. Moreover, by changing the reservoir rock wettability, asphaltene reduces the effective oil permeability and increases the amount of residual oil in porous media. Furthermore, change in the fluid viscosity should also be considered as a determining factor. This study aims to model asphaltene precipitation in the reservoir and evaluate this phenomenon's consequences regarding the effects on the wells' Productivity Index (PI). After developing a thermodynamic asphaltene model based on Cubic Peng-Robinson EOS, the fluid model was exported into a commercial compositional simulator using in-house PVT software. Besides, asphaltene behavior was described using the solid model. Then, the dynamics of the precipitated asphaltene were investigated using deposition, porosity reduction, permeability reduction, and viscosity change models in the mentioned simulator. Additionally, a sensitivity analysis was done to see how deposition model parameters and the production rate can probably affect the formation damage and final Wells' PI under natural reservoir depletion. Finally, the most significant parameters triggering asphaltene damage were identified. The results indicated that the damage triggered by asphaltene deposition, through plugging and decreasing porosity and permeability, and a change in viscosity was disclosed as a decline in wells' PI. The results also showed that although adsorption significantly affects the decrease in wells' PI, plugging is a more determining mechanism.

Keywords: Thermodynamic Model, Deposition Model, Compositional Simulator, Productivity Index.

Introduction
Asphaltene precipitation can result from changing the reservoir pressure (e.g., during natural depletion in under-saturated reservoirs or its fluid composition (e.g., during gas injection). It may bring about unpleasant conditions like reducing permeability and altering the wettability of reservoir rock toward oil wet [1].
Asphaltene can reduce the mobility of the reservoir fluid by altering the rock's wettability unfavorably or blocking the reservoir rock's pore throats. According to recent studies, the deposition would result in the most significant damage in the reservoir, especially in the vicinity of the production well, due to the severity of the pressure drop at this point [2]. Although some researchers assumed precipitated asphaltene would immediately deposit on the pore surface and not flow in the reservoir [3, 4], the opposite has also been reported [5]. A fraction of precipitated asphaltene would be adsorbed on the active sites of the surface due to formation-oil interactions or stops behind the throats. Continuous adsorption of asphaltene particles on pore surfaces narrows the pores. As a result, the higher flow velocity can remove deposited asphaltene from the surface whenever it goes beyond a critical velocity [6].
As mentioned earlier, the net asphaltene deposition volume results from three main mechanisms: surface adsorption, pore throat plugging, and entrainment of deposited asphaltene. Plugging occurs when the asphaltene particles are greater than the rock pore throats.
Reservoir flow is affected by the asphaltene phenomenon in a couple of ways. These effects may be modeled through variations of some rock and fluid properties such as porosity, permeability, viscosity, and wettability [7]. Ali and Islam concluded that while adsorption affects only wettability, it does not change the formation permeability. On the other hand, the deposition determines the extent of permeability damage [8]. Iwere et al. utilized the laboratory data to simulate the asphaltene precipitation in fractured reservoirs using the Eclipse100 simulator. Results obtained from both experiments and representative models showed that asphaltene precipitation rigorously depends on the type of lithology and pore

**Corresponding author:* Sedigheh Izadi, Engineering Department, National Iranian South Oil Company, Ahwaz, Iran
E-mail addresses: sedighehizadi.83@gmail.com
Received 2021-08-02, Received in revised form 2023-02-21, Accepted 2023-02-25, Available online 2023-05-24

throat size, which form the porosity-permeability combination. So, as the pore throat gets smaller, the tendency of the precipitated asphaltene for blockage increases. Permeability decreases with pressure reduction because of the asphaltene precipitation. Still, the significant result was that the same amount of asphaltene for two crude oils did not have the same permeability reduction due to the different pore architecture. Also, it has been shown that acidizing, as a fracturing technique, can cause a chemical reaction with carbonated rock and produce carbon dioxide, which can, in turn, lead to increased asphaltene deposition. [9]. Dehghani et al. showed that depending on reservoir rock type, the level of acidity (fluid type), the nature of porous media, and the adsorption of asphaltene flocculated particles results in a significant reduction in porosity and permeability [10]. Mirzabozorg et al. through a numerical study of asphaltene deposition in a fractured Iranian reservoir, concluded that increasing fracture spacing is associated with a decline in oil production rate and an increase in pressure drop, and this would result in increasing asphaltene deposition [11]. Usually, in asphaltene modeling studies, all the models based on which the asphaltene behavior in the reservoir is described, including changes in porosity, permeability, and rock wettability, are considered. Still, the most dominant damage mechanism is plugging the throats connecting pores by asphaltene particles and, thus, the reduction of rock permeability. Fadili et al. did an experimental and numerical study using the Eclipse simulator. Their results indicated that when bottom-hole pressure is high enough, the decline in production rate is not significant near the onset pressure and vice versa [12]. The asphaltene onset pressure is the pressure that corresponds to the start of asphaltene precipitation at the reservoir temperature. According to Khanifar et al. oil recovery decreases by 3.6 percent in an asphaltic oil reservoir under natural depletion. Their study also showed that precipitation and permeability reduction parameters could affect oil recovery by decreases of mostly 4 and 2 percent, respectively. They observed the intensified effects in the average reservoir pressure, which was at least 100 and 50% of decrease for precipitation and permeability reduction, respectively [13]. Saeedi conducted a numerical study using experimental asphaltene precipitation data to show the effects of deposition parameters and production rate on asphaltene net deposition volume and formation damage. She concluded that increasing the flocculation rate increased deposition and permeability damage. Furthermore, surface deposition affects permeability and relative permeability more than plugging does. Moreover, under natural depletion, the higher the production rate, the higher the formation damage due to adsorption, plugging, and deposition mechanisms [14]. If we want to differentiate these three processes, adsorption occurs when trapped asphaltene fines are adsorbed onto the surface of the reservoir rock. In contrast, asphaltene flocs may deposit onto their surface during deposition. Meanwhile, the deposited flocs could be trapped in the pore spaces depending on their size (plugging) or returned to oil depending on local shear velocity (entrainment).

On the other hand, due to the entrainment mechanism, deposition volume and permeability damage decrease, and cumulative production and overall recovery increase. Where this mechanism is active, it's level increases along with decreasing the distance from the production well. In this study, it is illustrated that under natural depletion, the higher production rate, the lower oil relative permeability, and finally, by decreasing distance from the production well, the plugging rate and permeability damage increase due to higher pressure drop around the well.

Bagherzadeh et al. used the Eclipse simulator to assess the permeability reduction of sandstone and carbonate rocks using the power-law expression. Both simulated results of sandstone and carbonate rocks matched the experimental data only in the final stages of the injected pore volume. This difference is related to considering the adsorption and plugging coefficient in simulation, which may not exist at first. Moreover, in carbonate analysis, the entrainment mechanism resists more permeability reduction and cannot improve permeability in contrast with experimental data. Sensitivity analysis showed that adsorption and plugging govern asphaltene deposition mechanisms at a low injection rate.

On the other hand, the entrainment mechanism is determinant at higher injection rates [15]. Ghadimi et al. studied the wettability change mechanism during asphaltene precipitation. They concluded that the wettability alteration is the leading cause of reduced well production rate by asphaltene deposition in the reservoir. Their results also disclosed most of the asphaltene deposits around the well at the beginning of production. But this is not true when time passes, and the maximum deposition occurs unexpectedly at the furthest distance from the well [16]. Therefore, it emphasizes the importance of time as a determining factor in the asphaltene net deposition volume.

To calculate the precipitated asphaltene fraction, the phase behavior of asphaltene must be determined first. To date, different thermodynamic models have been proposed in various research to do so. A few researchers considered a colloidal model and irreversible precipitation for asphaltene [17], while others considered solubility models and reversible precipitation processes [18]. The solubility model of Flory-Huggins, Cubic-EOS, and dense-liquid fluid theories (CEOS, CPA, and PC-SAFT EOSs) is based on the idea of asphaltene precipitation reversibility [19]. The approaches based on the association equation of state, such as CPA and PC-SAFT, which are taken advantage of for the multicomponent multiphase compositional models of asphaltene precipitation, take much more computational expense than CEOS [20], [21]. Yan et al. investigated the feasibility of association-based equations of state in compositional simulators. He discovered that PC-SAFT EOS's processing time was at least three times SRK [22].

Moreover, molecular characterization of heavy components is not done precisely enough by PC-SAFT, which may lead to significant errors in simulation results. On the other hand, the results' accuracy of the solid model compared with PC-SAFT has been demonstrated to be in the same range. Nevertheless, the PC-SAFT model indicates a better match with empirical data. In the case of such data scarcity, PC-SAFT delivers better predictions of asphaltene behavior than cubic EOS [23].

So far, the effect of the asphaltene precipitation phenomenon Still, they have hardly presented a validity check for their numerical model as the basis of their further calculations

and analyses. Moreover, in this study, a solid model with sufficient accuracy was built and exported into the suitable simulator by an in-house PVT software to take advantage of this simulator's capabilities for modeling the decline in wells' PI, which is only due to asphaltene precipitation phenomenon, regardless of other phenomena. Furthermore, no recent research has studied the effects of the asphaltene phenomenon on PI of production wells in such detail. Therefore, a complete detailed framework has been proposed for asphaltene modeling through conducting this research, which could benefit future researchers in this area.

In the present work, an oil sample from one of Iranian South oil naturally fractured reservoirs is thermodynamically modeled. The fluid and asphaltene precipitation behavior is described using a Peng-Robinson EOS and a solid model. Next, numerical simulation of precipitation and deposition processes is accomplished using a compositional simulator to study how the asphaltene deposition in the reservoir affects the wells' performance. As a result, porosity/permeability reduction and viscosity change are modeled numerically. Meanwhile, asphaltene is considered a component(s) that can precipitate depending on their weight percentage in the solution. Next, the asphaltene simulation model is validated, and a sensitivity analysis is conducted to identify the most critical parameters of the asphaltene model.

Materials and Methods

Fluid Model

The phase behavior of reservoir fluid depends on its composition, pressure, and temperature. Fluid properties are necessary for the simulator to predict its thermodynamic behavior under various reservoir conditions. Consequently, a precise fluid model is an important prerequisite for accurate simulation results. In this study, the fluid model was created using WinProp. The fluid sample was taken from an under-saturated fractured oil reservoir. Reservoir fluid components are shown in Table 1. The oil gravity is 31.23 o API. The initial reservoir pressure and temperature are 7448 psi and 250 °F, respectively. on reservoir performance has been investigated numerically by several researchers.

The PR-EOS was used to model fluid behavior: During this matching process, Tc, Pc, acentric factor, molecular weight, volume shift, omega A and omega B parameters were used as tuning parameters to model the fluid behavior at the initial reservoir conditions. The basic form of Peng-Robinson EOS is as below [24]:

$$P = \frac{RT}{v-b} = \frac{a}{(v+b)(v+b+2c)(v-b)} \quad (1)$$

The energy parameter of each component is calculated by:

$$a_i = \Omega_a = \frac{R^2 T_{ci}^2}{P_{ci}} a(T_{ri}) \quad (2)$$

Table 1 Reservoir fluid composition and properties

Component Name	Mole fraction	MW	Tc (R)	Pc (psia)
N2	0.001	28.013	227.16	492.314
CO_2	0.033702	44.01	547.56	1069.865
H_2S	0.017202	34.08	671.76	1296.182
CH_4	0.440135	16.043	343.08	667.196
C2H6	0.089207	30.07	549.72	708.344
C3H8	0.054104	44.097	665.64	615.76
IC4	0.011001	58.124	734.58	529.054
NC4	0.030302	58.124	765.36	551.098
IC5	0.010301	72.151	828.72	490.844
NC5	0.011401	72.151	845.28	489.375
FC6	0.033102	86	913.5	477.03
FC7	0.035003	96	977.76	455.133
FC8	0.013701	107	1026.9	427.946
FC9	0.025402	121	1077.3	395.909
FC10	0.019302	134	1119.78	367.546
FC11	0.018502	147	1158.48	340.505
C12-C17	0.062226	198.35	1298.85	291.472
C18-C22	0.032493	338.402	1501.507	203.161
C23-C28	0.024592	295.922	1478.091	211.331
C29-C34	0.014821	471.807	1425.993	170.34
C35	0.001819	470.965	1438.883	160.261
C36A+	0.019962	582.883	1808.83	130.933
C36B+	0.00721	641.437	1698.121	125.836

$$a(T_{ci}) = [1 + a_0\left(1 - \sqrt{T_{ri}}\right) + a_1 + a_2\left(1 - T_r\right)\left(0.7 - T_r\right)]^2 \quad (3)$$

where a_1 and a_2 are zero for hydrocarbon (non-polar) components. For the Peng-Robinson equation, a_0 can be obtained by:

$$a_0 = \left(0.3764 + 1.5422\omega_i - 0.2699\omega_i^2\right),\ \omega \le 0.49 \quad (4)$$

$$a_0 = \left(0.379642 + 1.4850\omega_i - 0.164423\omega_i^2 - 0.016666\omega_i^3\right),\ \omega \ge 0.49 \quad (5)$$

$$b_i = \Omega_b = \frac{R^2 T_{ci}^2}{P_{ci}} - C_i \quad (6)$$

where *ci* is the volume shift parameter of component i, for the Peng-Robinson: Ω_a = = 0.457236, Ω_b = 0.077796. The dimensionless volume shift is defined as:

$$S_i = \frac{c_i}{b_i + c_i} = \frac{c_i}{\Omega_a \frac{RT_{ci}}{P_{ci}}} \quad (7)$$

S_i values are determined by matching experimental density data at Tr= 0.7 for many components, and the s value is stored in the simulation. If these values are not available, the parameters for light components are calculated using Peng-Robinson EOS:

$$s_i = 0.4772w_i - 0.154700 \quad (8)$$

For the heavy components, this parameter is obtained by matching their specific gravity (SG) at standard conditions. Binary Interaction Parameters (BIP) are usually calculated by parametrizing EOS. The other method for doing so was proposed by Mehra and Li [24]:

$$d_{ij} = \left[1 - \left(\frac{\sqrt{v_{ci}^{1/3} v_{ci}^{1/3}}}{v_{ci}^{1/3} + v_{ci}^{1/3}}\right)\right]^n \quad (9)$$

where n=1 and v_{ci} is the critical molar volume of component *i*, critical pressure, and temperature of heavy components were among the regression variables to match the thermodynamic behavior of the sample fluid. Table 1 also shows predicted PVT properties for the reservoir fluid. Matching fluid expansion test results are shown in Figure 1.

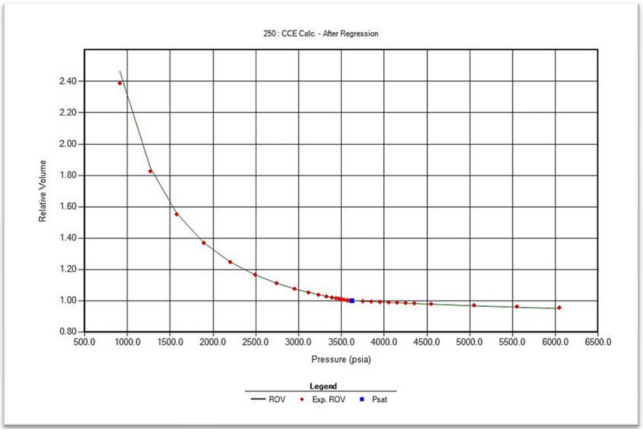

Fig. 1 Matching the CCE test results for the fluid sample at reservoir temperature (in WinProp).

This figure displays a schematic of matching Constant Composition Expansion (CCE) test results.

As regards the asphaltene precipitation, asphaltene precipitation is modeled using a multiphase flash calculation. The fluid phases are described with a cubic equation of state, and the fugacity of components in the solid phase is predicted using the CEOS (solid model). The precipitated phase is an ideal mixture of solid components [24]. After calculating the asphaltene mole fraction by empirical asphaltene content, the same critical properties and acentric factors are assigned to the B+ component. Still, different interaction parameters with the components C_1 to C_5 are required.

Therefore, a second-time regression is needed to ensure the accuracy of the fluid modeling results. Now, it is time for the calculation of reference fugacity. But why is reference fugacity needed?

At the beginning of flash calculation and during conducting a stability test, it is found that the hydrocarbon fluid is divided into two phases, and as a result,

$$\ln f_{io} = \ln f_{ig},\quad i = 1,\ldots,nc \quad (10)$$

This equation suggests that the fugacity of solid components in both the oil and gas phases is equal. It is true with this assumption that there is no asphaltene in the gas phase, but this is not the case for the asphaltene one. With such a limiting condition (Eq.10), the hydrocarbon system (vapor-liquid or just liquid) is observed until another solid phase appears. If s1 represents the solid phase in equilibrium with the liquid and gaseous hydrocarbons, and the asphaltene fugacity in the liquid phase exceeds that of pure asphaltene ($f_{nco} > f_{s1}$), then the asphaltene would precipitate. The equation for phase equilibrium would be as follows:

$$\ln f_{nco} = \ln f_{s1} \quad (11)$$

that expresses the equality of fugacity of the precipitating component in the oil phase, and the precipitated solid s1. The fugacity of components in the hydrocarbon (including oil and gas phases) is calculated by the Peng-Robinson EOS, and the fugacity of solid S1 would be as follows:

$$\ln f_{s1} = \ln f_{s1}^* + \frac{V_{s1}(P - P^*)}{RT} \quad (12)$$

According to this thermodynamic equilibrium equation (Eq. 12), the precipitation process of s1 is thermodynamically reversible. Therefore, solid s1 can return to solution whenever the system is outside the asphaltene precipitation envelope [25].

Central to modeling asphaltene precipitation is solids characterization, whether in a solution or solid phase. Moreover, the binary interaction between the hydrocarbon light components and the asphaltene component significantly affects the asphaltene precipitation curve- the greater value for BIP, the higher amount of asphaltene precipitation [24]. The reference fugacity and BIP were used to match the asphaltene precipitation data best. Fluid components and calculated volume fraction of the asphaltene component are shown in Table 1. SARA test analysis was also available for this oil sample. According to this test, asphaltene in the dead oil is 0.56 wt. %. The asphaltene content was measured by the IP-143 method (n-heptane insoluble asphaltene). Figure 2 shows the asphaltene precipitation curve generated by WinProp.

Finally, after checking PVT parameters to keep a good

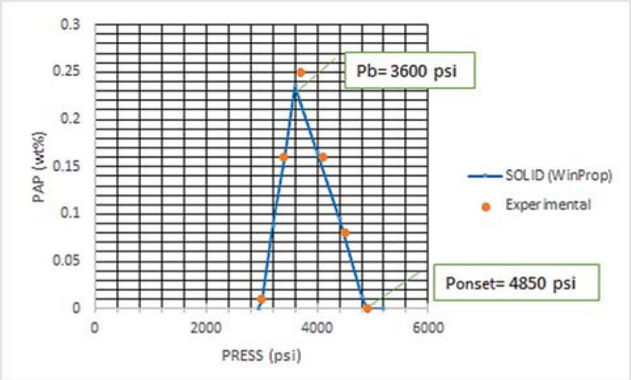

Fig. 2 Asphaltene precipitation curve by WinProp. As it is clear, the Percentage of Asphaltene Precipitation (PAP) is close to the experimental one. Furthermore, predicted Asphaltene Onset Pressure (AOP) has been obtained.

match after asphaltene modeling, this model was exported into the E300 by PVTPro (Figure 3). This check was done after exporting the fluid model into PVTPro, too. Note that the asphaltene model in E300 assumes the same molecular characteristics for the heaviest fluid component and asphaltene. Therefore, it would cause some uncertainty in the final simulation results. In this research, we removed the source of this error by building an asphaltene thermodynamic model in WinProp to find more accurate characteristics for the asphaltene component. Then the results were manually imported into E300. Another motivation for doing in WinProp was to use its results in a future comparative study between GEM and E300 simulators.

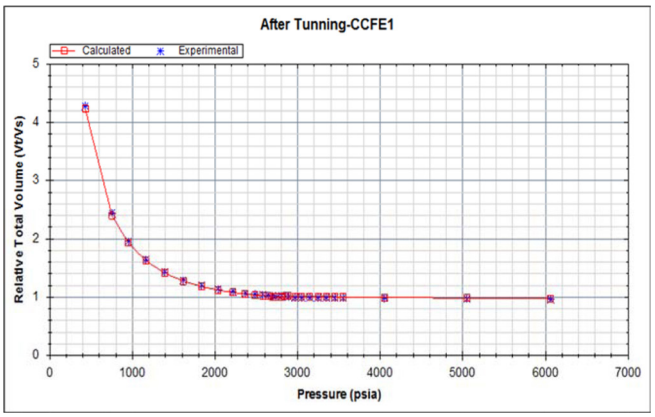

Fig. 3 Matching the CCE test results for the fluid sample (in PVTPro). The fluid model previously built by WinProp was imported into PVTPro and exported to provide E300 with a compositional format of the fluid model.

Asphaltene model

The complexity of natural fractures and their network is combined with the unknown nature of the asphaltene behavior. It renders numerical simulation of this phenomenon complicated in unconventional low permeability tight reservoirs.

A sector 3D model was developed for our study based on the real data that the Bangestan study group reported simulating asphaltene precipitation occurrence and its negative consequences in that reservoir [26].

Asphaltene modeling consists of four different stages:

where the double arrow represents the reversibility of the process (partially or totally). Precipitation would be followed by the subsequent processes of flocculation, deposition, and damage, which in turn includes a viscosity effect, as follows [26].

Precipitation -Dissolution

The asphaltene content could be either dissolved in oil or precipitated.

In this study, asphaltene was modeled as a pure solid. First of all, to calculate the amount of asphaltene precipitate, the heaviest pseudo-component ($C36^{+}$) was split into two non-precipitating ($C36A^{+}$) and precipitating ($C36B^{+}$) components (Table 1). Then, critical properties were calculated by the Lee-Kesler equation. To avoid losing the accuracy of results, unnecessary components for asphaltene modeling are not lumped together.

In E300, the precipitation process takes place based on its calculations:

Below is the formula based on which the simulator determines whether the asphaltene precipitates or remains finely dissolved [26]:

$$X_{\lim}=\frac{W_{\lim}}{100}.\frac{m_{woil}}{m_{wp}x_p} \tag{13}$$

where w_{lim} is the maximum dissolved asphaltene in oil (wt. %). It is represented here as the maximum amount of asphaltene that can exist in dissolved form. m_{woil} (Dimensionless), m_{wp} (Dimensionless) and x_p (fraction) are the oil and asphaltene molecular weight (dimensionless) and mole fraction of precipitation component (fraction), respectively. Accordingly, if the resulting mole fraction for the precipitation component is less than this limit, the precipitation component would remain in the solution, and there would be no fines. But if the mole fraction of this component exceeds this value, the dissolved and fine fractions of the precipitation component would be as follows [26]:

$$X_{pd}=X_{\lim} \tag{14}$$

$$X_{pf}=X_p-X_{\lim} \tag{15}$$

The result of this section was entered manually into the model.

Flocculation- Dissociation

During this stage, the settled particles from the precipitation stage join together and form larger particles called flocs. As the name suggests, this process is the exact opposite of flocculation, which can occur or not depending on whether the user allows the reversibility of the flocculation process during the simulation (In this study, the process was assumed to be irreversible, so no dissociation rate was determined).

The following formula represents a model by which it is possible to calculate how fast the flocculation would occur after precipitation:

$$R_a=\frac{\partial C_a}{\partial t}=r_{ia}C_i-r_{ai}C_a \tag{16}$$

where R_a is the rate of flocs aggregation (dimensionless), C_i is the concentration of the fines (dimensionless), C_a is

the concentration of the flocs (dimensionless), r_{ia} and r_{ai} are the aggregation rate coefficient for fines (1/day) and the dissociation rate coefficient for flocs (1/day), respectively [26].

Deposition-Entrainment

Deposition occurs when the flocs are exchanged between the oil phase and the surface of the reservoir rock. The flocs can adsorb on the surface of the rock, can be trapped within the porous media and plug the pore throats, or can be entrained and returned to the oil phase because of high local velocity (in the deposition area).

In the current compositional simulator, the net deposition rate in the flow direction i would be described as follows [26]:

$$\frac{\partial \varepsilon_i}{\partial t} = \frac{\alpha}{d}\phi C_a + \gamma_1 \left| F_{oi} \right| C_a - \beta\left(\left| U_{oi} \right| - U_{cr}\right)^+ \varepsilon_i \quad (17)$$

where ε_i denotes the amount of deposition in i flow direction (fraction), α represents the adsorption coefficient (1/day), d is the number of dimensions (1, 2, or 3), Φ is porosity (fraction), C_a is volume concentration of the flowing flocs (dimensionless), γ_1 is the plugging coefficient (1/ft^3), F_{oi} is the oil flowrate (ft^3/day), β is the entrainment coefficient (1/ft), Uoi is the oil Darcy velocity(ft/day), and U_{cr} is the critical velocity (ft/day) [26].

Note that the input parameters, β, γ_1, and Ucr are user-input parameters and should be obtained from core flood experiments.

Note that the total volume fraction of asphaltene deposits would be the sum of the deposits in each direction i [26].

Asphaltene Damage

In the solid deposition model, the reduction in fluid volume is modeled through oil saturation and, consequently, porosity which is directly related to saturation. In the current simulator, the porosity is controlled by the asphaltene deposition rate:

$$\phi = \phi_0 - \int_0^t \frac{d\varepsilon}{dt} dt \quad (18)$$

Where ϕ_0 denotes porosity at the zero time step (fraction), and ε represents the volume of the asphaltene deposit (fraction) [26].

The effects of asphaltene deposition on permeability can be modeled in two ways:

It can be correlated to porosity using a power-law correlation that relates present absolute permeability with this parameter in the previous time step:

$$\frac{K}{K_0} = \left(1 - \frac{\varepsilon}{\phi_0}\right)^{\delta} \quad (19)$$

where k and k_0 are permeability (mD) at times t and t_0, respectively, and δ is a user input parameter (dimensionless) that comes from core flood experiments [26].

Another option is to provide a table containing permeability multipliers versus the volume fraction of asphaltene deposit (this option is preferred in this study. Note that the data for this section were taken from the literature since there was no permeability damage data for this reservoir) [26].

Furthermore, in this simulator, the change in viscosity can be modeled by using three options, all of which make use of a parameter called *mass fraction of asphaltene precipitate*, including both fines and flocs, C_p:

$$C_p = \frac{m_{wp} X_{pf} + m_{wf} x_f}{m_{woil}} \quad (20)$$

The first model is the Generalized Einstein model:

$$\frac{\mu}{\mu_0} = 1 + aC_p \quad (21)$$

where μ_0 denotes the oil viscosity (c_p) at C_p=0 (this was the choice for this study with the default value for *a*, which is equal to 2.5).

The Krieger and Dougherty model is also available that takes two parameters of μ_0 and η (intrinsic viscosity), where C_{p0} is the maximum packing concentration [26]:

$$\frac{\mu}{\mu_0} = \left(1 - \frac{C_p}{C_{p0}}\right)^{-\eta C_{p0}} \quad (22)$$

Third, viscosity could be similarly modeled using a table consisting of a viscosity multiplier for each value of the mass fraction of the asphaltene precipitate at a specific pressure step [26].

One more thing is that, by attaching to the reservoir rock, asphaltene flocs might change rock wettability from water-wet to oil-wet. Although, the effect of wettability change can be partially illustrated through a change in the relative permeability of rock from a water-wet system to an oil-wet one [26], which can be evaluated for a two-phase flow state. However, in this study, since the aquifer is small, it was assumed that there would not be a significant water influx into the reservoir. Therefore, fluid flow toward the production well was considered a single phase. As a result, wettability alteration was not considered in this study.

Simulation Model

A 3D Cartesian grid was developed for an unconventional under-saturated fractured reservoir producing under natural depletion. The data of one of the fractured reservoirs in south-western Iran was used to create this reservoir model. The main production mechanism of this reservoir is rock and fluid expansion. The 3D grid discretization is shown in Figure 4. The initial reservoir conditions have been specified in Table 2, and the overall grid description can be seen in Table 3.

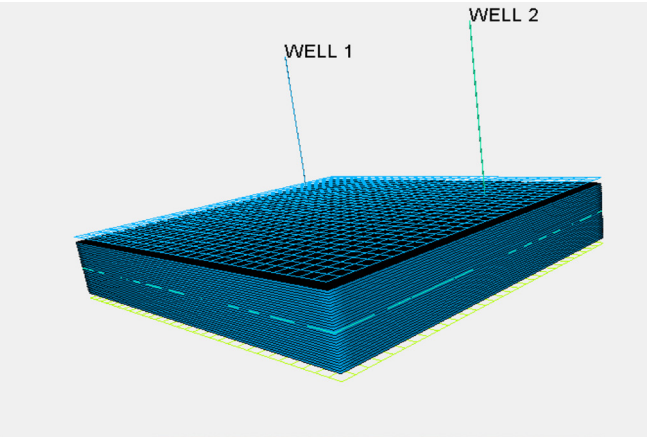

Fig. 4 The 3D reservoir discretization in the Cartesian system (because the history matched model was unavailable, a sector model was created and used instead).

Table 2 Simulation Sector model input data.

Property	value
Matrix Porosity(fraction)	0.034
Fracture Porosity (fraction)	0.001
Matrix K_h (mD)	0.0186
Fracture K_h (mD)	100
Matrix K_v (mD)	0.0073
Fracture K_v (mD)	20
Matrix block height (ft)	20
Sigma (ft^{-2})	0.05
Rock Compressibility (Psi^{-1})	3e6-
Saturation Pressure (Psi)	3597
Initial reservoir pressure (Psi)	7448
Present reservoir pressure (Psi)	5450
Reservoir temperature (^{0} F)	250
Water-oil contact (ft)	15355
No. of SCAL & PVT (-)	1

Table 3 Characteristics of sector model.

Feature	Characterization		
Number of grid blocks	X	Y	Z
	30	30	30(60)
No. of wells	2		
Wells locations in the reservoir	NE / NW		
OIP	2.46e8		
Aquifer	1-AQUCT		
Hysteresis	SATOPTS/HYSTER		
Prediction time interval	30 Years (2020-2050)		

Two production wells were considered in two different corners of the reservoir with a minimum bottom-hole pressure of 3900 psi. The initial reservoir pressure and temperature are 7448 psi and 250 °F, respectively. The predicted onset pressure at this temperature is 4850 psi (Figure 2). Since there wasn't any experimental upper onset pressure, it was predicted using WinProp for calibrating the simulation models in the following sections. As a result, we can see that the reservoir is not in the range of asphaltene precipitation yet. The parameters of the deposition model are also listed in Table 4. This data was taken from literature since they were unavailable for the present reservoir. In this section, the model (and data file) was created and saved in Petrel.

Validation of simulation model

In this stage, Petrel 3D model was run in E300 compositional simulator. Figure 5 shows the effect of asphaltene deposition on the average reservoir pressure. As it is clear, in the case of the asphaltic reservoir, the average pressure of the reservoir is much higher than that of the non-asphaltic reservoir, which is caused by the presence of more residual oil in the former (see Figure 6). Figure 6 illustrates how the cumulative oil production and productivity index of a well are affected by the asphaltene deposition and subsequent permeability reduction.

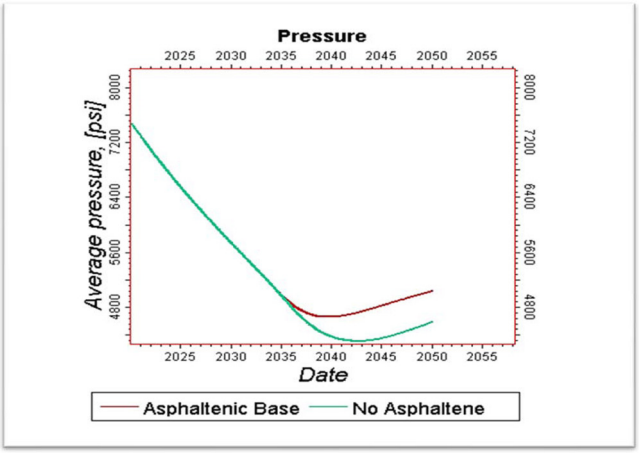

Fig. 5 Average reservoir pressure vs. time for two simulation cases: without asphaltene and asphaltic (As it is clear, the reservoir pressure is higher for the asphaltic one, and this is the primary stage of model validation).

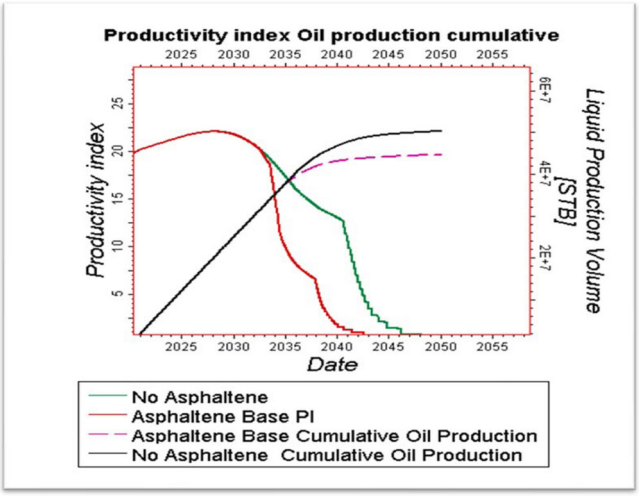

Fig. 6 Cumulative oil production and PI vs. time for two simulation cases: without asphaltene and asphaltic case. It is observed that PI and cumulative oil production decrease with asphaltene deposition. It is what we expect in a valid asphaltene model.

Table 4 Characteristics of sector model.

Parameter	Value (min)	Value (max)	unit
Flocculation rate	0.01	0.01	(1/day)
Deposition rate coefficient (α)	0.0001	0.1	(1/day)
Plugging coefficient (γ)	0.00001	0.01	($1/ft^3$)
Entrainment coefficient (β)	1	0	(1/ft)
Critical velocity (Ucr)	0	2500	(ft/day)
The slope of relative viscosity concerning concentration for the Einstein Model	2.5	2.5	dimensionless

In the asphaltic case, both permeability reduction and viscosity change contribute to changing the well's productivity. Wettability alteration has not been investigated here. Both the productivity index and cumulative oil decrease with the asphaltene deposition. In Figure 7, it can be seen how the production rate of well#1 decreases due to asphaltene deposition. Sometimes, although pressure decline and all the other negative consequences of asphaltene precipitation are observable during reservoir production, there might be an inaccurate onset pressure or even an incorrect asphaltene mole fraction. It has been checked for this simulation model (Figure 8) to ensure that all the results are reliable enough for further analysis. It is illustrated in two fracture blocks, one near the production well and the other far from the well. As soon as block pressure drops below the onset pressure, the asphaltene mole fraction gets non-zero until it reaches its maximum value. This model was obtained using the correct table illustrated in Table 5 as the asphaltene weight percentage in the simulation study.

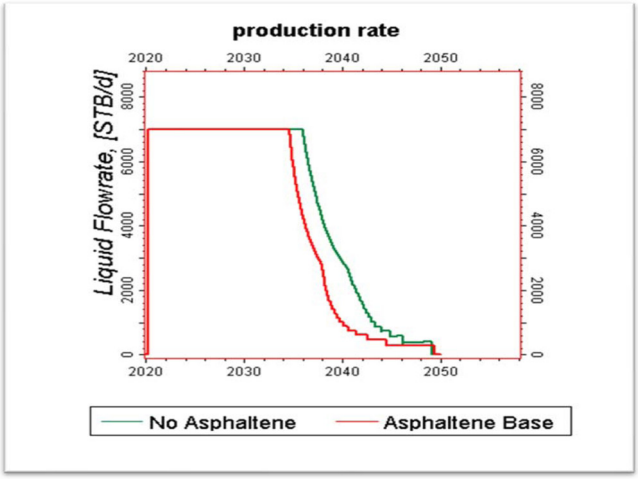

Fig. 7 Decreasing production rate of well#1 due to asphaltene presence. It can witness the effect of asphaltene precipitation being considered in a simulation model.

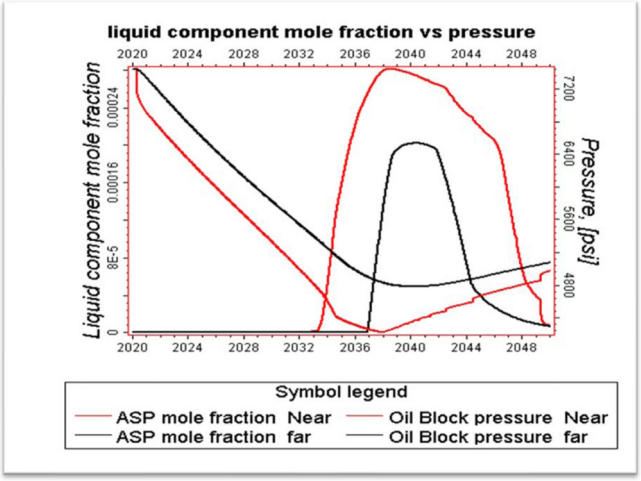

Fig. 8 Asphaltene component mole fraction vs. time and pressure for two blocks: near the production well and far from it (to confirm the validity of the asphaltene simulation model for the Asphaltene Onset Pressure (AOP) and asphaltene weight percent).

Table 5 Data used to adjust the onset pressure and asphaltene precipitation.

Pressure (psi)	Dissolved asphaltene in the oil phase (%)
3700	0.16
4100	0.25
4500	0.33
4550	0.339
4600	0.34
4650	0.36
4700	0.37
4750	0.38
4800	0.39
4850	0.41
7000	0.41
10000	0.41

The onset pressure at which asphaltene content would reach its maximum in crude oil plays an essential role in tuning the base simulation model.

Moreover, this study emphasizes the permeability damage, only caused by asphaltene precipitation and not a mix of other factors contributing to declining the reservoir & well pressure. Based on this, the asphaltene model was validated using a simple test involving running the model with an only-precipitation scenario. In other words, during asphaltene precipitation, there should not be any change in permeability and bottom-hole pressure due to this phenomenon. Therefore, two asphaltenic and non-asphaltenic simulation cases should display the same pressure behavior during reservoir depletion (Figure 9), as it is not the case for other simulators used to model asphaltene precipitation like GEM [27].

The final result of this section was a compositional simulation model that was saved as a data file to be used as the basis of sensitivity analysis. Moreover, manually, the results which were imported into E300 are seen in Tables 4 and 5.

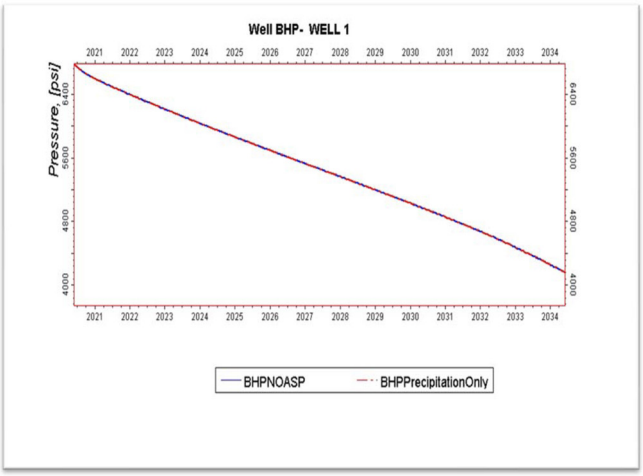

Fig. 9 Comparing bottom-hole pressure in two simulation cases: no asphaltene and precipitation–only asphaltic. The same pressure behavior in both cases indicates that any change in pressure during asphaltic reservoir simulation is only due to the asphaltene phenomenon and not any other factor.

Productivity Index Calculation

Engineers define Productivity Index (PI) to define how a well and reservoir communicate. PI of a well, which is defined as the ratio of the total rate of well liquids to the pressure drop and is denoted by the symbol J, for a water-free production would be as follows:

$$J = \frac{Q_p}{P_d - P_w} \tag{23}$$

where Q_p is the rate of production for the phase p, and P_d is drainage area pressure:

Considering steady-state radial flow in the drainage area and taking the connection transmissibility factor of the well into account:

$$T_{wj} = \frac{c\theta kh}{\ln(r_o / r_w) + s} \tag{24}$$

where c is a conversion factor (0.001127 in field units), θ is the angle of the segment connecting with the well, Kh is the effective permeability capacity of the connection, and ro is the pressure equivalent radius of grid block, and S denotes the skin factor.

Then, for a vertical well, we will have:

$$J = \sum_j [T_{wj} M_{P,j} (\frac{\ln(r_o / r_w) + s}{\ln(r_d / r_w) + s})] \tag{25}$$

where $\sum_j$ denotes a summation of all the connections of the well for the simulator, T_{wj} is the connection factor of the well, and M_{Pj} is phase mobility.

The drainage radius (*rd*) is not usually known accurately. In this simulator, an option sets this parameter equal to the value equivalent to grid block pressure for each connection. Therefore, this equation is reduced to the following form:

$$J = \Sigma_j [T_{wj} M_{p,j}] \tag{26}$$

And hence, the PI should be regarded as the PI of the well within its connecting grid blocks instead of its drainage area [26].

It is assumed that the reservoir will remain under-saturated during natural depletion, and the only active mechanism contributing to production is rock and fluid expansion. Therefore, water cut would be at most 30%, and wells no. 1 and 2 produce a daily rate of 7000 and 5000 STB/day. The flow is assumed to be steady-state and radial toward the well. Furthermore, since the reservoir is fractured, the most influential blocks of the grid, based on which analyses are done, are located in the fracture section of the grid. Note that in this study, the effect of porosity reduction and hence, the impact of pressure decline on permeability due to this phenomenon has not been considered. Therefore, damaged permeability is merely the product of asphaltene precipitation occurrence. It is also supposed that there was a single-phase flow due to the small size of the aquifer. Finally, the effect of time and size of the reservoir on asphaltene deposition and damage has been ignored in this study.

Results and Discussion

As mentioned earlier, the deposition model consists of some parameters, and each might contribute differently to the net asphaltene deposition. Therefore, a sensitivity analysis was done to study the effect of each parameter on the net asphaltene deposition volume, consequently permeability & PI change. These parameters include an adsorption coefficient (α), a plugging coefficient (Y_1), an entrainment coefficient (β), and critical velocity (U_{cr}). Note that since the weight percentage of asphaltene is negligible in this case, high orders of difference have been considered for sensitivity analysis on each parameter to see the effect more clearly. Note that the data for these asphaltene-controlling parameters have been taken from the literature (Table 4).

Figure 10 shows the effect of the adsorption coefficient on the net deposition volume fraction, permeability reduction, and block pressure. Figure 11 and Figure 12 represents the same effect on well#1 PI and production rate. Therefore, it can be concluded that this parameter, which indicates the amount of asphaltene adsorption, will not significantly affect the asphaltene deposition volume and therefore, the well productivity index. Figure 13 demonstrates the far more positive effect of reducing the *plugging coefficient* on both the asphaltene deposition volume and the level of reservoir permeability damage compared to alpha.

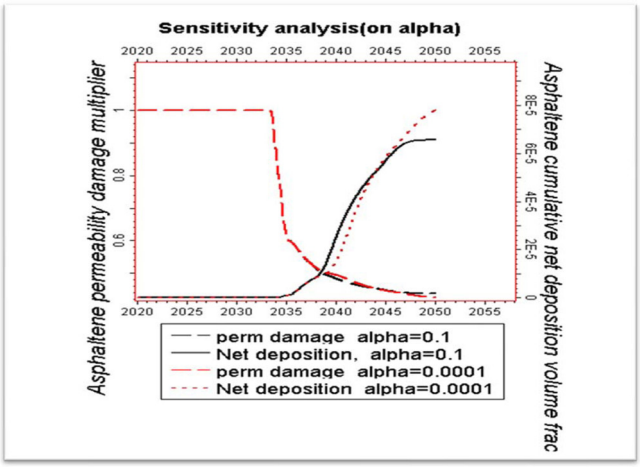

Fig.10 The effect of decreasing adsorption coefficient on the asphaltene net deposition volume and permeability damage. The level of asphaltene adsorption does not cause significant damage to the reservoir.

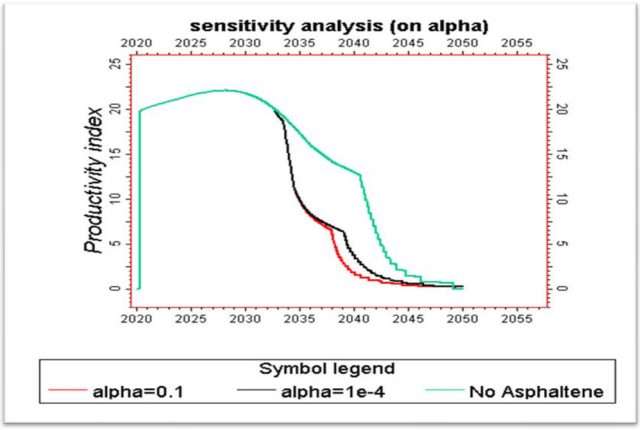

Fig. 11 The effect of decreasing adsorption coefficient on well#1 PI (It is not affected considerably by the asphaltene adsorption).

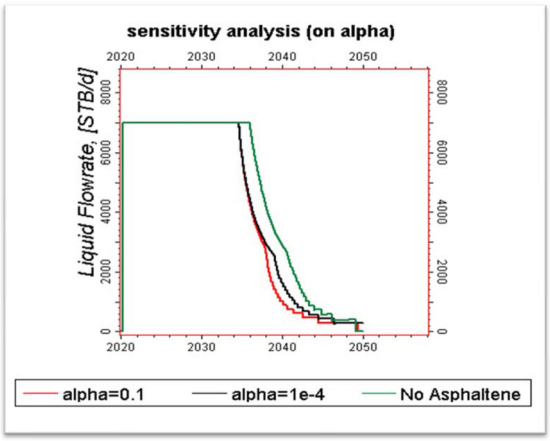

Fig. 12 The effect of decreasing the asphaltene adsorption coefficient on well#1 production rate (Apparently, it is not affected significantly by the asphaltene adsorption).

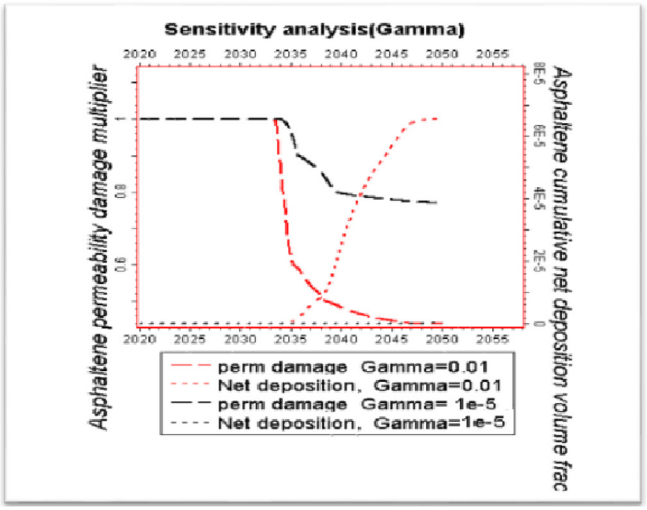

Fig. 13 The positive effect of reducing plugging coefficient (Y_1) on the asphaltene net deposition volume and permeability damage (This reduction in plugging has noticeably led to more minor formation damage).

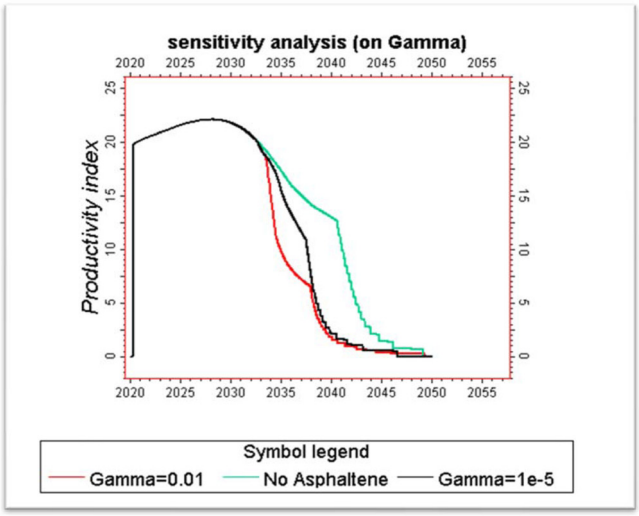

Fig. 14 The positive effect of reduction in plugging coefficient (Y_1) on well#1 PI (It can be concluded that during asphaltene deposition, well PI can increase with decreasing the level of plugging in pore throats)..

This effective change can be better seen in Figure 14, which suggests that wells' PI could be strongly affected by blockage of the rock pore throats during asphaltene deposition in the reservoir. It is because when there is not much plugging, there would be a later drop in the bottom-hole pressure, and subsequently, the production rate starts to decline at a later time (Figure 15). This is due to a sharp decrease in the net volume of asphaltene deposition.

Two other parameters of the deposition model, entrainment coefficient and critical velocity, are closely related. Therefore, their sensitivity has been done simultaneously (Figures 16 - 18). Critical velocity is the determining factor. Therefore, if the fluid velocity exceeds the critical velocity, oil flow can carry the deposited asphaltene particles and prevent permeability damage [8]. For studying the effect of these two parameters, From Figures 16 - 18, it can be inferred that when critical velocity decreases to below a specific amount (we assumed zero for this study), the entrainment mechanism becomes active. As a result, there would be a significant decrease in the level of permeability damage and also in the net deposition volume.

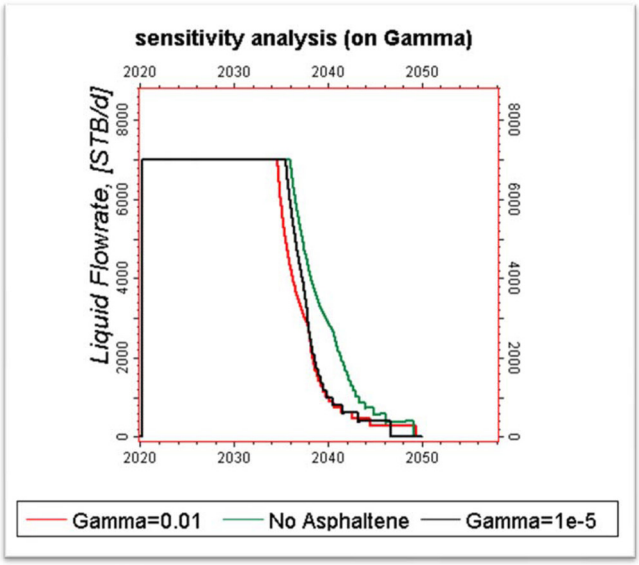

Fig. 15 The effect of reduction in plugging coefficient (Y_1) on well #1 Flow rate. It is clear that when plugging intensity is less, the production rate reduction is delayed.

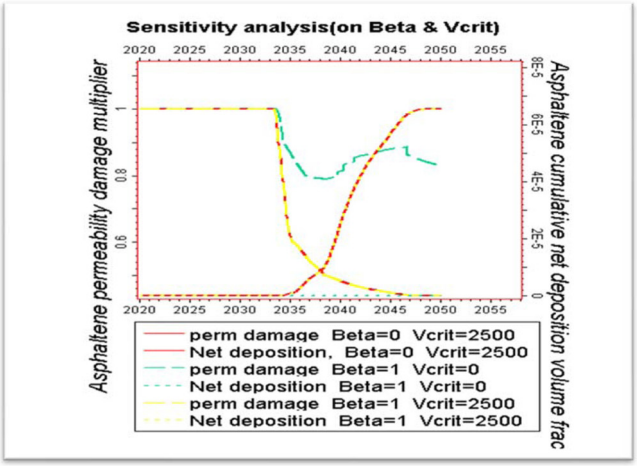

Fig 16 The effect of increasing the entrainment coefficient (β) and reducing critical velocity on asphaltene net deposition volume and permeability damage (significant decrease in permeability damage is observed when beta increases and critical velocity decreases).

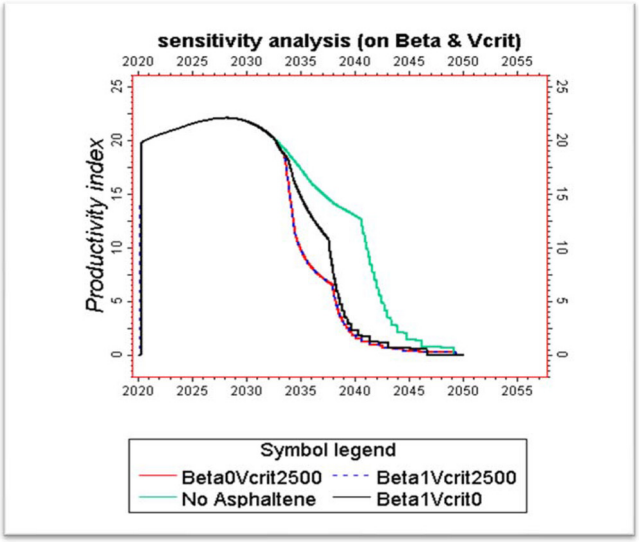

Fig. 17 The positive effect of increasing entrainment coefficient (β) and decreasing critical velocity on well#1 PI. (The black curve in this figure; Accordingly, a lower critical velocity/ higher fluid velocity could compensate for the adverse effects of asphaltene deposition on wells' PI).

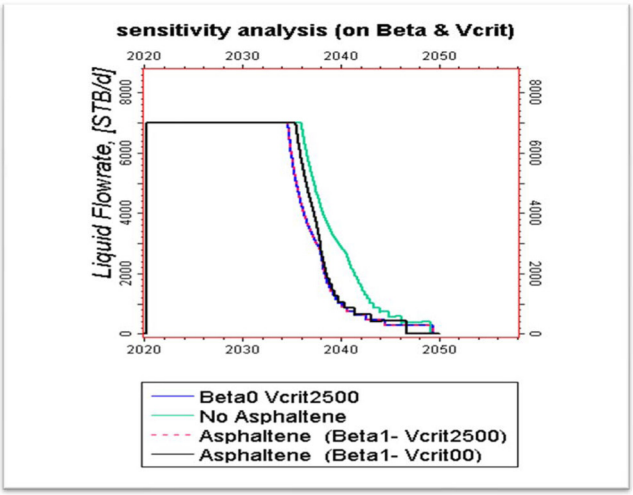

Fig. 18 The effect of increasing entrainment coefficient (β) and decreasing critical velocity on well#1 production rate. It is seen that critical velocity reduction leads to an increase in the production rate, which is due to asphaltene entrainment phenomenon.

On the contrary, when the critical velocity is high enough (here, the simulator default is used, 2500), although the beta parameter is set to maximum, entrainment becomes zero. Therefore, it coincides with the base case where the beta coefficient is 0. Subsequently, there would be minor permeability damage because of the entrainment activity near the wellbore, where fluid velocity is high enough owing to a smaller cross-section than regions away from the wellbore. Figure 17 explains the positive effect of the lowest possible critical velocity on well# PI. Figure 19 proposes that the higher the production rate, the higher the net deposition volume and permeability damage because of the higher intensity of pressure drop around the well location. It may happen simultaneously with an earlier pressure drop below the asphaltene onset pressure.

Additionally, with a higher production rate, more asphaltic oil passes through the formation. Consequently, more asphaltene precipitates and deposition occur earlier than expected for a given production rate—finally, higher net deposition volume at the end of the wells and reservoir's life. Figure 20 compares well#1 PI in two different production rates and demonstrates the lower PIs for well producing at higher rates.

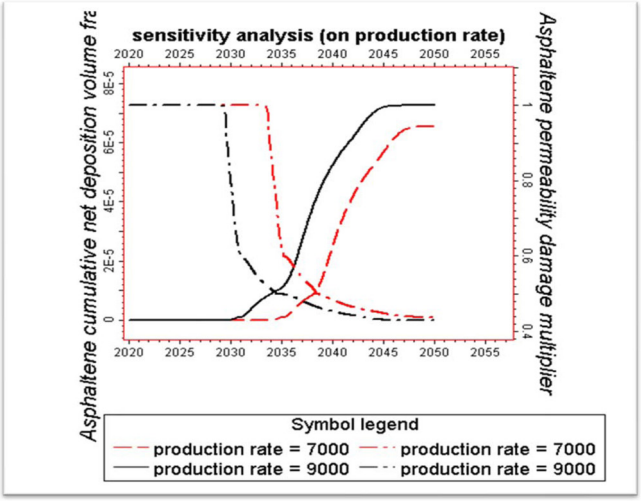

Fig. 19 The effect of increasing production rate on the asphaltene net deposition volume and permeability damage (well#1). That is, the higher the production rate, the more severe the formation damage.

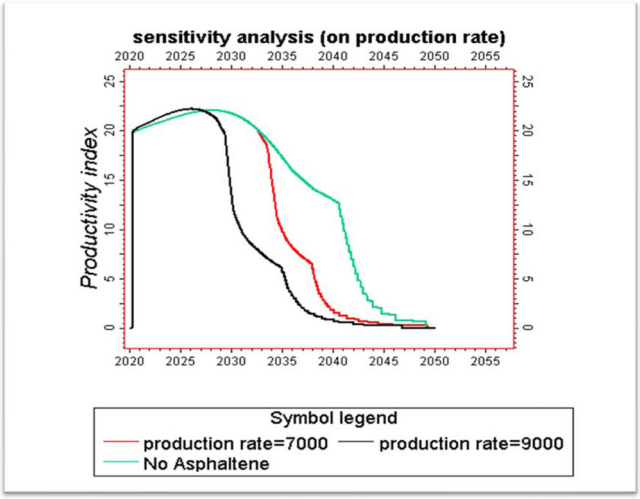

Fig. 20 The effect of increasing production rate on well#1 PI in two asphaltic simulation cases vs. a non-asphaltic one. The reduction of well PI is getting worse with increasing its production rate.

In this case, although there is a higher depletion rate, intensified pressure drop exceeds this rate increase, and PI decreases eventually.

Figure 21 compares two mechanisms contributing to changing the reservoir flow: viscosity and permeability. In this case, the decrease in permeability can cause a sharper decrease in the wells' PI compared to the change in viscosity.

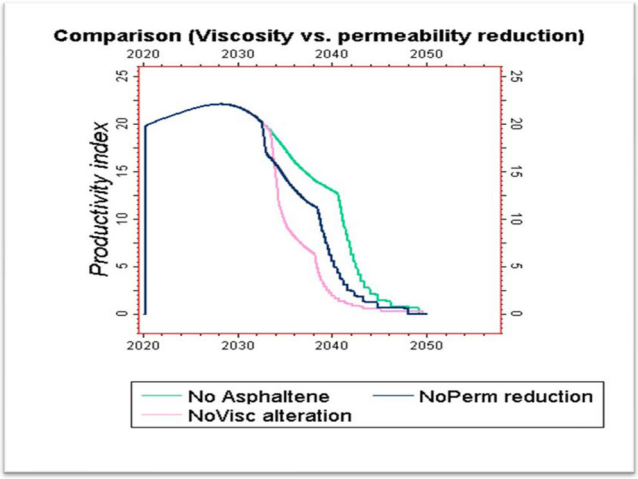

Fig. 21 Comparing the contribution of two separate mechanisms of only permeability reduction and only viscosity change to the decrease in PI in the asphaltic simulation case. It is seen that permeability reduction plays a significant role in damaging the reservoir during asphaltene precipitation.

Conclusions

In this research, asphaltene modeling was conducted using a commercial compositional simulator to address the problems likely encountered during the natural depletion of a tight fractured oil reservoir. Porosity, permeability, and viscosity change models were utilized, while precipitated asphaltene was assumed to be a pure solid component. A table proportionate to the asphaltene deposited volume was used for permeability reduction in the base model during the implementation of sensitivity analysis. The final results of this study indicated that during natural depletion, the highest asphaltene deposition volume and permeability damage occur in the vicinity of the wellbore. Also, the effect of permeability reduction and viscosity change was investigated separately. Comparing the results show that permeability alteration is the leading cause of reducing wells' productivity indices compared to viscosity alteration. The sensitivity analysis on deposition model parameters indicated that there would not be considerable permeability damage with a smaller adsorption coefficient. Still, there would be less drop in a well PI and production rate. This effect is not as much as a small enough plugging coefficient since, according to this study's findings, it contributes more to the negative consequences of asphaltene deposition. of course, the lowest critical velocity and an entrainment coefficient of near unity could have the same desirable results as a small gamma to reduce the intensity of permeability damage and improve well PI and production rate. Additionally, it was demonstrated that a high production rate could lead to a higher net asphaltene deposition volume and, eventually, a lower well PI. Finally, it was figured out that permeability reduction plays a more critical role in reducing the wells' PI than viscosity alteration.

Nomenclatures

W_{lim} = maximum dissolved asphaltene in oil, wt. %
m_{woil}= oil and asphaltene molecular weight, dimensionless
m_{wp}= asphaltene molecular weight, dimensionless
x_p = mole fraction of precipitation component, dimensionless
R_a = rate of flocs aggregation, dimensionless
Ci = concentration of fines, dimensionless
Ca = concentration of the flocs, dimensionless
r_{ia} = aggregation rate coefficient for fines, 1/day
r_{ai} = dissociation rate coefficient for flocs, 1/day
k_{12} = forward rate of solid s2 formation from s1 , day-1
k_{21} = reverse rate of formation of solid s1 from s2, day-1
r = reaction rate, day-1
C_{s1o} = concentration of suspended solid s1 in oil phase, mol/m^3
$C_{s2,o}$ = concentration of suspended solid s2 in oil phase, mol/m^3
ε_i = the amount of deposition in i flow direction, fraction
α = adsorption coefficient, 1/day
d = number of dimensions (1, 2, or 3)
Φ = porosity, fraction
Ca = volume concentration of the flowing flocs, dimensionless
γ_1 = the plugging coefficient, 1/ft3
F_{oi} = oil flow rate, ft^3/day
β = entrainment coefficient, 1/ft
U_{oi} = oil Darcy velocity, ft/day
U_{cr} = critical velocity, ft/day
ε = volume of asphaltene deposit, fraction
k = k0 permeability at times t, mD
k_0 =permeability at time t0, mD
δ = a user input parameter that comes from core flood experiments, dimensionless
V_{ci} = critical molar volume of component i
Cp = mass fraction of asphaltene precipitate, wt. %
μ_0 = oil viscosity at Cp=0, cP
η = intrinsic viscosity, cP
C_{p0} = maximum packing concentration,
S_{ocra} and S_{ocri} = critical oil in water saturations, fraction
S_{wcra} and S_{wcri} = critical water saturations, fraction
k_{rwa} = oil-wet relative permeability to water, mD
k_{rwi} = water-wet relative permeability to water, mD
wt. %.= weight percent of asphaltene, percent
Tc= Critical temperature, 0F
Pc= critical pressure, psi
MW= molecular weight, dimensionless
CCE= constant composition test
ci = volume shift parameter of component i, dimensionless
Si= volume shift parameter, dimensionless
Ωa= energy parameter of component shift
Ωb= energy parameter of component shift

References

1. Nasrabadi H, Moortgat J, Firoozabadi A (2016) New three-phase multicomponent compositional model for asphaltene precipitation during CO_2 injection using CPAEOS, Energy and Fuels, 30, 4: 3306–3319, doi. org/10.1021/acs.energyfuels.5b02944.
2. Mohebbinia S, Sepehrnoori K, Kazemi Nia Korrani A, T Johns R (2014) Simulation of Asphaltene precipitation during gas injection using PC-SAFT EOS, Journal of

Petroleum Science and Engineering, 158, 693-706, doi.org/10.2118/170697-MS.
3. Fazelipour W, Pope G A, Sepehrnoori K (2008) Development of a fully implicit, parallel, EOS compositional simulator to model asphaltene precipitation in petroleum reservoirs. In: SPE Annual Technical Conference and Exhibition, Society of Petroleum Engineers, doi.org/10.2118/120203-STU.
4. Gonzalez Abad K G (2013) Development of a compositional reservoir simulator for asphaltene precipitation based on a thermodynamically consistent model, Doctoral Thesis, Texas A&M University.
5. Nghiem L X, Kohse B F, Ali S, Doan Q (2000) Asphaltene precipitation: phase behaviour modelling and compositional simulation, In: SPE Asia Pacific Conference on Integrated Modelling for Asset Management, Society of Petroleum Engineers, OnePetro, doi.org/10.2118/59432-MS.
6. Gruesbeck C, Collins R (1982) Entrainment and deposition of fine particles in porous media. Soc. Petrol. Engineering Journal, 22, 06: 847–856, doi.org/10.2118/8430-PA.
7. Fadili A, Alizadeh N, Leung E, Khaksar A, Ashoori A (2009) Simulating the permeability reduction due to asphaltene deposition in porous media, International Petroleum Technology Conference, Doha, Qatar, 8-9, IPTC 2009, cp-151, doi.org/10.3997/2214-4609-pdb.151.iptc13262.
8. Muhammad Ashraf A, Muhammad R I (1998) The Effect of asphaltene precipitation on carbonate rock permeability: an experimental and numerical approach, SPE Prod and Fac, 13, 03: 178–183, https://doi.org/10.2118/50963-PA.
9. Iwere F O, Apaydin O G, Moreno J E, Schlumberger, Ventura R L, Garcia J L, Penox E P (2002) Simulation of asphaltene precipitation inn fractured reservoirs, A Case Study, doi:10.2118/74373-MS.
10. 10. Mousavi Dehghani A, Vafaie M, Mirzayi B, Fasih M (2007) Experimental investigation on asphaltene deposition in porous media during miscible gas injection, Journal of Chemistry and Chemical Engineering, 26, 4: 39-48, DOI: 10.30492/IJCCE.2007.7599.
11. Mirzabozorg A, M B, Kharrat R, Abedi J, Ghotbi C (2009) Simulation study of permeability impairment due to asphaltene deposition in one of the Iranian Oil Reservoir, the Canadian International Petroleum Conference, Calgary, Alberta, June, PETSOC-2009-088, https://doi.org/10.2118/2009-088.
12. Yi T, Fadili A, Ibrahim M, Sulaiman Al-Matar B (2009) Modelling the effect of asphaltene on the development of the marrat field, SPE European Formation Damage Conference held in Scheveningen, The Netherlands, 27–29 May, doi.org/10.2118/120988-MS.
13. Khanifar A, Demiral B, Darman N (2011) The effect of asphaltene precipitation and control parameters on reservoir performance: a numerical approach, SPE Reservoir Characterisation and Simulation Conference and Exhibition Held in Abu Dhabi, UAE, 9–11, doi.org/10.2118/146188-MS.
14. Saeedi A (2013), Simulation of Asphaltene deposition mechanism in one of Iranian South reservoirs using E300 Simulator, MSc thesis, Sahand University of Technology, 1-98.
15. Bagherzadeh H, Rashtchian D, Ghazanfari M H, Kharrat R (2014) A core scale investigation of asphaltene precipitation during simultaneous injection of oil and CO_2: an experimental and simulation study, Energy Sources, Part A, 36: 1077–1092, doi.org/10.1080/15567036.2010.551261.
16. Ghadimi M, Amani M J (2019) Modelling of formation damage due to asphaltene deposition in near wellbore region using a cylindrical compositional simulator, Journal of Petroleum Science and Engineering, 173: 630-639, https://doi.org/10.1016/j.petrol.2018.10.058.
17. Abedini A, Ashoori S, Torabi F, Saki Y, Dinarvand N (2011) Mechanism of the reversibility of asphaltene precipitation in crude oil, Journal of Petroleum Science and Engineering, 78, 2: 316–320, doi.org/10.1016/j.petrol.2011.07.010.
18. Pedersen K S, Christensen P L, Shaikh J A (2010) Phase Behavior of Petroleum Reservoir Fluids, CRC Press.
19. Li Z, Firoozabadi A (2010) Cubic-plus-association equation of state for asphaltene precipitation in live oil. Energy Fuels, 24, 5: 2956–2963, doi.org/10.1021/ef9014263.
20. Mohebbinia S, Sepehrnoori K, Kazemi Nia Korrani A, Johns T R (2014) Simulation of asphaltene precipitation during gas injection using PC-SAFT EOS, Journal of Petroleum Science and Engineering, 158, 693-706, doi.org/10.2118/170697-MS.
21. Daryasafar A, Masoudi M, Kord Sh, Madani M (2020) Evaluation of different thermodynamic models in predicting asphaltene precipitation: a comparative study, Fluid Phase Equilibria, 514: 112557, doi.org/10.1016/j.fluid.2020.112557.
22. Yan W, Michelsen M L, Stenby E H (2011) On application of non-cubic EoS to compositional reservoir simulation, SPE EUROPEC/EAGE Annual Conference and Exhibition. Vienna, Austria, May. Society of Petroleum Engineers, doi.org/10.2118/142955-MS.
23. Abouie A, Darabi H, Sepehrnoori K (2017) Data-driven comparison between solid model and PC-SAFT for modeling asphaltene precipitation, Journal of Natural Gas Science and Engineering, 45, 325–337, doi.org/10.1016/j.jngse.2017.05.007.
24. Computer Modelling Group Ltd. (CMG) (2015) WinProp User's Guide: Advanced Phase Behaviour and fluid property simulator, Calgary, Canada, The user's guide is available internally in the CMG simulator.
25. Kohse B F, Nghiem L X (2004) Modelling asphaltene precipitation and deposition in a compositional reservoir simulator, fourteenth symposium on improved oil recovery held in Tulsa, Oklahoma, U.S.A., 17–21 doi.org/10.2118/89437-MS.
26. Eclipse Technical Description, 2013.1: Asphaltene Option, Aphaltene formation: Pre-2011 Model.
27. Izadi S, Jafarzadegan M (2021) Comparison of asphaltene models in two commercial compositional simulators, Journal of Petroleum Science and Technology 11, 4: 43-54..